

Binary caesium–lanthanum oxide supported on MCM-41: A new stable heterogeneous basic catalyst

K. R. Kloetstra, M. van Laren and H. van Bekkum

Laboratory of Organic Chemistry and Catalysis, Delft University of Technology, Julianalaan 136, 2628 BL Delft, The Netherlands

Heterogeneous mesoporous stable basic catalysts have been prepared by wet or solid-state impregnation of MCM-41 with caesium acetate and lanthanum nitrate followed by thermal decomposition. ^{133}Cs MAS NMR data of CsLa/MCM-41 show an increase in the Cs–O bond length in the CsLa mixed oxides compared with that in Cs oxides supported on MCM-41. A small difference in chemical shift between the hydrated and dehydrated materials is observed, indicating a weak interaction of water with Cs^+ cations. CO_2 temperature-programmed desorption (TPD) suggests that these materials possess small oxide clusters of mild basicity. The thermal stability of the materials, which is independent of the framework aluminium content, is reflected by an unaffected CO_2 desorption and BET surface area on successive thermal cycles. Alkali metal–lanthanum binary oxides of the Na, K and Rb-type appear to be thermally less stable, in the sense of a significantly smaller CO_2 desorption indicative of particle clustering. ^{23}Na MAS NMR shows several resonances for the NaLaO_x materials. The presence of the single Rb-oxide component in the RbLaO_x materials is confirmed by ^{87}Rb MAS NMR. The mild base strength of the CsLaO_x/MCM-41 is demonstrated by its ability to remove a proton from enolates having a $\text{p}K_{\text{a}} \leq 10.2$. The presence of lanthanum and the mesoporous framework govern the activity and product selectivity in the liquid-phase Michael addition of ethyl cyanoacetate to ethyl acrylate. The Knoevenagel addition of enolates to benzaldehyde in aqueous media is also catalysed by the CsLa-oxide/MCM-41 system. The catalyst is re-usable after regeneration at high temperature without loss of activity.

Heterogeneous base catalysis is a growing field of interest.¹ Alkaline earth metal oxides, rare earth metal oxides, special zeolites and clays have been used as base catalysts.^{1,2} The zeolites are used generally in their alkali metal ion-exchanged form^{1–4} or serve as a support for small alkali metal oxide particles.^{1,2,5–11} The zeolitic systems are insensitive to carbon dioxide poisoning and are moderately moisture sensitive. However, a limitation of these microporous materials is the pore accessibility. The mesoporous molecular sieve MCM-41^{12,13} has proven to be a promising candidate for the catalytic conversion of large molecules.^{14,15} Sodium and caesium ion-exchanged MCM-41 is weakly basic;¹⁵ its basicity was improved by the introduction of intraporous caesium oxide particles.^{15,16} These strongly basic mesoporous systems are able to catalyse the Michael addition with enolates of a relatively weak acidity ($\text{p}K_{\text{a}} \leq 13.3$). The stability of these catalysts is rather poor which seems to hold generally for caesium oxide supported on molecular sieves containing a small amount of framework aluminium.^{10,16}

Binary oxides containing alkali metals might have interesting properties compared with the corresponding single oxide, for instance an increased stability and improved catalytic behaviour. Preparation of binary oxides and other related oxidic materials has been reviewed recently.¹⁷ Stable binary lithium–lanthanide oxides have been prepared *via* mixtures of their metal salts¹⁸ or *via* mixtures of the corresponding single oxides.¹⁹ Characterization of LiLnO₂ (Ln = La, Nd and Sm) after use in the oxidative coupling of methane (OCM) at 750 °C, revealed that the structure of these catalysts was retained.¹⁸ The yttrium analogue LiYO₂ appeared to undergo partial transformation into an amorphous phase at the reported reaction conditions.^{20,21} All the LiLnO₂ compounds showed interesting performances in OCM. The use of CsLaO₂ has not been reported. Like most of the binary alkali metal–lanthanum oxides, CsLaO₂ possesses a structure of the NaFeO₂ type,^{19,22} an ordered rock salt structure consisting of mixed cation layers of closest-packed O^{2-} .²³

Binary CsLa oxide supported on MCM-41 might have

interesting performances in base catalysed reactions like Michael addition. The objective of this work was to prepare a stable basic catalyst of the MCM-41 type by impregnation of stoichiometric amounts of caesium and lanthanum. The physicochemical properties of the intraporous caesium–lanthanum mixed-oxide particles were investigated by a variety of characterization techniques and by testing these composites in base-catalysed liquid-phase reactions. Binary alkali metal–lanthanum oxides containing sodium, potassium or rubidium were prepared in a similar way inside the MCM-41 material to study some properties of these composite systems and compare them with the caesium analogue.

Experimental

Catalyst preparation

The MCM-41 support was synthesized by mixing 16.8 g of TMA–SiO₂ solution [TMA/SiO₂ = 0.5; 10 wt.% SiO₂; tetramethylammonium hydroxide (TMAOH) was purchased from Aldrich and the silica source was Cab-osil M5 from Fluka] with 6.6 g of sodium silicate (Aldrich; 27 wt.% SiO₂). Subsequently 31 g of water and 4.6 g of silica were added to the mixture. Under vigorous stirring, 15.5 g of cetyltrimethylammonium bromide (ACROS) in 104 g of water were poured in the mixture. Finally the gel was enriched with the appropriate amount of sodium aluminate (Riedel-de Häen; 54% Al₂O₃ and 41% Na₂O) to obtain the desired Si/Al ratio. The gel was stirred for 2 h at room temperature and subsequently kept, without stirring, in an oven at 100 °C overnight. The resulting solid was filtered and washed thoroughly with water, dried at 90 °C under vacuum and calcined at 540 °C in air for 10 h.

MCM-41 samples containing only one of the metals caesium or lanthanum, denoted Cs/MCM-41 or La/MCM-41, respectively, were prepared by stirring 1.0 g of MCM-41 in a solution containing the appropriate amount of caesium acetate (CsOAc; ACROS) or lanthanum nitrate hexahydrate (Merck) in 4 g of methanol for 3 h at 60 °C. The solvent was removed

quickly under vacuum in a rotary evaporator and the materials were subsequently calcined at 500 °C for 5 h in air.

CsLa/MCM-41 materials, containing equimolar amounts of both caesium and lanthanum, were prepared in three different ways, namely (i) one-step wet impregnation, (ii) one-step solid state impregnation and (iii) two-step wet impregnation. The first method involved stirring 1.0 g of MCM-41 in a methanolic solution containing equimolar amounts of CsOAc and $\text{La}(\text{NO}_3)_3 \cdot 6\text{H}_2\text{O}$ for 3 h at 60 °C, followed by drying quickly and subsequent calcination at 500 °C for 5 h in air. These samples will be denoted CsLa/MCM-41A.

The second way involved solid-state impregnation. The MCM-41 support was ground carefully with the appropriate amounts of CsOAc and $\text{La}(\text{NO}_3)_3 \cdot 6\text{H}_2\text{O}$ and the mixture was calcined at 500 °C (1 °C min⁻¹ heating rate) for 5 h in air. These samples will be denoted CsLa/MCM-41B.

The third route involved first preparing monometallic lanthana-containing MCM-41 (La/MCM-41; see above) and subsequently impregnating this with CsOAc and calcining the materials again at 500 °C. These materials are denoted CsLa/MCM-41C. All the CsLa/MCM-41 materials were loaded with ca. 5 wt.% caesium and 5 wt.% lanthanum.

The Na and Cs ion-exchanged MCM-41 samples (Na-MCM-41 and Cs-MCM-41, respectively) were prepared according to ref. 14 by using aqueous NaCl (Baker) or CsCl (ACROS).

All-silica NaLa/MCM-41, KLa/MCM-41 and RbLa/MCM-41 were prepared in a similar way to the first method, namely by using stoichiometric amounts of the corresponding alkali-metal acetate and lanthanum nitrate hexahydrate (based on 5 wt.% La).

Bulk CsLaO₂ was prepared by mixing the appropriate amounts of CsOAc and $\text{La}(\text{NO}_3)_3 \cdot 6\text{H}_2\text{O}$ in an alcoholic solution at room temperature for a few hours followed by drying and calcining at 500 °C for 5 h. This binary oxide showed diffraction peaks corresponding with literature data.²⁴ Binary MLaO₂ or M₂O–La₂O₃ (M = Na, K or Rb) was prepared in a similar way. Reference caesium oxide and lanthana were purchased from Aldrich.

Characterization

Structural characterization was performed by powder X-ray diffraction on a Philips PW 1840 diffractometer using monochromated Cu-K α radiation. Patterns were recorded from 1° to 40° (2 θ) with a resolution of 0.02° and a count time of 1 s at each point.

Differential scanning calorimetry with thermogravimetry (DSC–TG) was carried out with an STA-1500 H thermobalance (PL Thermal Sciences). Experiments were performed at a heating rate of 10 °C min⁻¹ in an air flow of ca. 50 ml min⁻¹.

Solid-state 52.5 MHz ¹³³Cs MAS NMR spectra were recorded at room temperature on a Varian VXR-400S spectrometer, equipped with a Doty Scientific Instruments 5 mm solids MAS probe. A recycle delay of 0.5 s, an acquisition time of 0.3 s and short 2.5 μs (ca. $\pi/5$) pulses, a spectral width of 100 kHz and a spin rate of 4–7 kHz were applied. The lines were referenced to a 1 M solution of CsCl in water ($\delta = 0$).

Recording of solid-state 105.5 MHz ²³Na MAS NMR spectra and 130.6 MHz ⁸⁷Rb MAS NMR spectra was performed in a similar way. For both nuclei a recycle delay of 2.0 s, an acquisition time of 0.3 s and short 2.0 μs pulses were used. The resonances were referenced to a 1 M solution of NaCl or RbCl ($\delta = 0$), respectively.

Temperature-programmed desorption (TPD) of carbon dioxide was performed on a Micromeritics 2900 TPD/TPR instrument. The calcined materials were first activated at 600 °C for 5 h and subsequently cooled to 110 °C under a helium flow. Then the activated materials were saturated with

dry gaseous carbon dioxide at this temperature. Physisorbed carbon dioxide was removed by purging the sample under a helium flow at 110 °C until a stable baseline was monitored (ca. 0.5 h). The TPD was performed under a helium flow (10 ml min⁻¹) by heating the sample from 110 to 600 °C with a heating rate of 10 °C min⁻¹.

Multipoint BET surface areas, pore volumes and pore size distributions of the materials were calculated from N₂ adsorption–desorption isotherms at –196 °C using a Quantochrome Autosorb 6 apparatus. The samples were outgassed for 16 h under vacuum at 350 °C prior to use.

Catalytic testing

The Michael additions were carried out as follows. A round-bottomed flask containing a mixture of 10 mmol of ethyl cyanoacetate, 10 mmol of ethyl acrylate (or another α,β -unsaturated ester), internal standard and 20 ml of ethanol was heated to reflux. At $t = 0$ the metal oxide containing MCM-41 (5% m/m with respect to the total amount of reactants) was added to the stirred mixture. The course of the reaction was monitored by GC (CP sil 5CB column). The products were identified by GC–MS, ¹H NMR and ¹³C NMR.

The Knoevenagel condensations were done in the same way, with 10 mmol of benzaldehyde instead of ethyl acrylate and 30 ml of solvent. The solvents used were ethanol or mixtures of H₂O–THF = 1 : 1 (THF = tetrahydrofuran) or H₂O–dioxane = 1 : 1.

Results and Discussion

Preparation and structural characterization of CsLa/MCM-41

The MCM-41 supported binary caesium–lanthanum oxides were prepared *via* three different routes (see Experimental). To study any influence of the framework aluminium content on the stability on the impregnated materials, MCM-41 materials with three different Si/Al ratios (15, 30 and ∞) were used. The first method, *via* a one-step wet impregnation in methanol, yielded an intraporous homogeneously dispersed binary CsLa oxide after calcination. In a separate experiment it was found that an equimolar mixture of caesium acetate and lanthanum nitrate after calcination gave the colourless binary mixed oxide CsLaO₂.²² When the molar amounts of caesium acetate were less than the molar amounts of lanthanum nitrate the same CsLa mixed oxide was formed along with lanthana (confirmed by ¹³³Cs MAS NMR). Larger amounts of caesium acetate give CsLaO₂ and Cs₂(CO₃)₂. The classical preparation method for CsLaO₂ is mixing stoichiometric amounts of Cs₂O with La₂O₃ and heating this mixture at 550 °C.^{19,22} Other binary alkali metal–lanthanide oxides can be prepared *via* thermal decomposition of the corresponding metal salts and resulted in the same binary oxide product as *via* the normal route.^{18,19,21,22}

The second route in loading the MCM-41 with oxides is by a solid state-like impregnation at 500 °C.^{25–27} In this way oxides disperse spontaneously on the internal surface of zeolites and MCM-41. Theoretically it should also be possible to impregnate MCM-41 with an equimolar mixture of caesium acetate and lanthanum nitrate by using this technique. To investigate whether it is possible to prepare intraporous dispersed caesium oxide particles on a lanthanum oxide layer, MCM-41 was also impregnated in two steps. Lanthana tends to spread in a monolayer on silica after thermal decomposition of the silica impregnated lanthanum nitrate salt.²⁸ The first step is loading MCM-41 with the lanthanum nitrate and subsequently calcining the material. The achieved intraporous lanthana possesses a high degree of lattice disorder which leads to a very active oxide.¹⁹ The last step is impregnating the LaO_x loaded material with caesium acetate and calcining

it again. Methanol was used as a solvent for all the wet impregnations. Loading MCM-41 with a larger salt content resulted in disruption of the MCM-41 framework structure probably owing to too strong interactions of the impregnated compounds.¹⁷ It was observed that when these experiments were done in water the MCM-41 framework structure was destroyed by the low pH caused by ionization of hydrated lanthanum cations.

Powder X-ray diffraction was carried out on the original MCM-41 supports and the calcined impregnated MCM-41 materials to examine the crystallinity of the impregnated MCM-41 materials. Fig. 1A, E and I show the X-ray diffractograms of the original supports. There is an increase in 'crystallinity' of the three parent MCM-41 supports with increase in the Si/Al ratio.^{29,30} All-silica MCM-41 seems to be less stable with respect to the one-step wet impregnation compared with the aluminosilicate MCM-41, which is reflected in

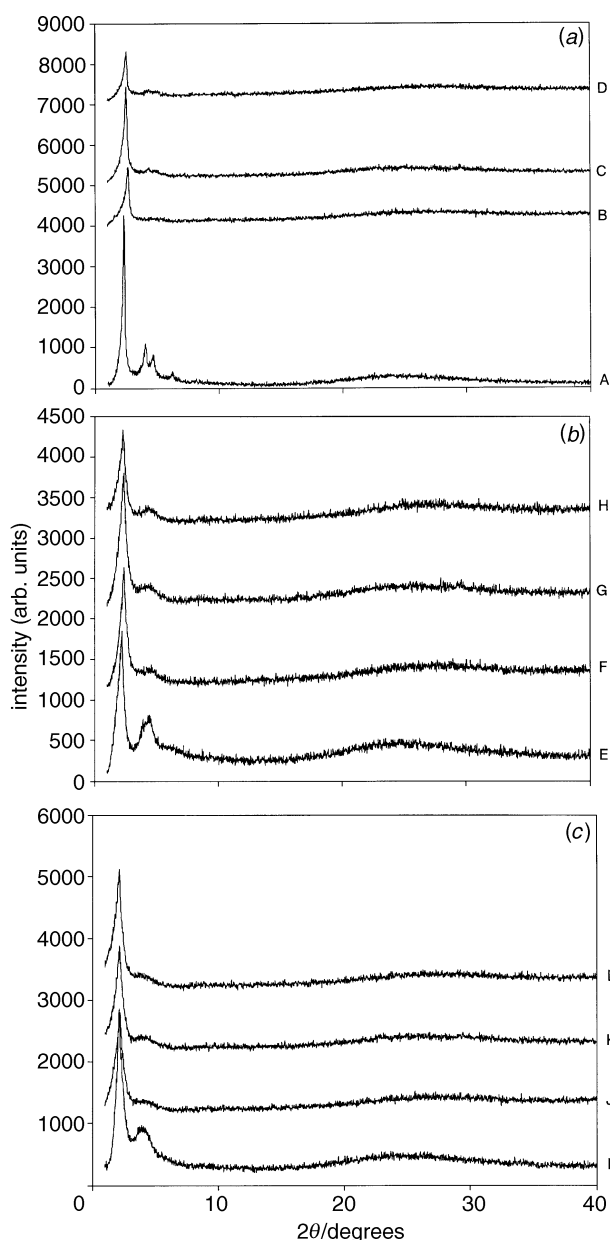


Fig. 1 X-Ray powder diffractograms of various CsLa/MCM-41 samples and their parent support (lowest pattern). In each box the second pattern is associated with method A, the third pattern is associated with method B and the upper pattern is associated with method C. A–D all-silica MCM-41 materials; E–H are MCM-41 materials with Si/Al = 30; I–L are MCM-41 materials with Si/Al = 15.

the decrease of intensity of the d_{100} -spacing by a factor of 3 (Fig. 1B). We note that a decrease in X-ray peak intensity is not necessarily an indication of a partial collapse or a lower regularity of the unidimensional pore arrangement.^{31,32} Also consideration is given to the high electron density of Cs^+ and La^{3+} loaded molecular sieves when using X-ray diffraction.⁵ Variation in peak intensities in the X-ray diffractograms has also been observed for caesium oxide-loaded zeolite, X.⁷ The all-silica MCM-41 support displays a better resistance to the solid-state impregnation treatment (Fig. 1C). This phenomenon is also observed for the other two MCM-41 supports (Fig. 1G and K). The effect of the two-step wet impregnation on the crystallinity is somewhat comparable with the one-step impregnation. Again, the two aluminosilicate MCM-41 samples show the largest preservation of the hexagonal ordering of the framework (Fig. 1D, H and L). X-ray crystalline CsLaO_2 is not observed in any of the impregnated MCM-41 materials whatever the technique used. This shows that the critical dispersion capacity of CsLaO_x on the surface of MCM-41 is not exceeded.²⁴

The adsorption–desorption isotherms of nitrogen on the original all-silica MCM-41 and the corresponding impregnated $\text{CsLaO}_x/\text{MCM-41}$ materials are illustrated in Fig. 2. The inflection point of the parent MCM-41 becomes less sharp and shifts to lower relative pressure indicating the creation of smaller mesopores by the impregnation. The decrease in adsorbed nitrogen, expressed as volume per mass unit, should therefore be considered with care. The preservation of the mesoporous framework structure of the samples $\text{CsLa}/\text{MCM-41B}$ and $\text{CsLa}/\text{MCM-41C}$, mentioned earlier, is indicated by the shape of the isotherms. The overall influence of the impregnation steps and the calcination treatment on the pore size, pore volume and BET area is summarized in Table 1. The large BET surface area of all the $\text{CsLa}/\text{MCM-41}$ materials is retained after re-evacuation at high temperature indicating intraporous thermally stable oxide clusters. This contrasts with the reported instability of the $\text{Cs}/\text{MCM-41}$ after a second heat treatment.¹⁶ The decrease in the cumulative mesopore volume and pore size (d_p) is in accord with the presence of the oxide particles inside the pores.^{33,34} The pore size is actually the mean Broekhoff–de Boer diameter assuming cylindrical pores²⁸ which appeared in earlier studies to give a reliable pore dimension.^{35,36}

Fig. 3 shows the DSC–TG behaviour of $\text{CsLa}/\text{MCM-41A}$, an all-silica MCM-41 loaded with caesium acetate and lanthanum nitrate *via* the one-step wet impregnation. A clear exotherm occurs at *ca.* 375 °C probably from the decomposition of caesium acetate.⁵ The gradual weight loss between 400 and 600 °C might stem from the endothermic decomposition of

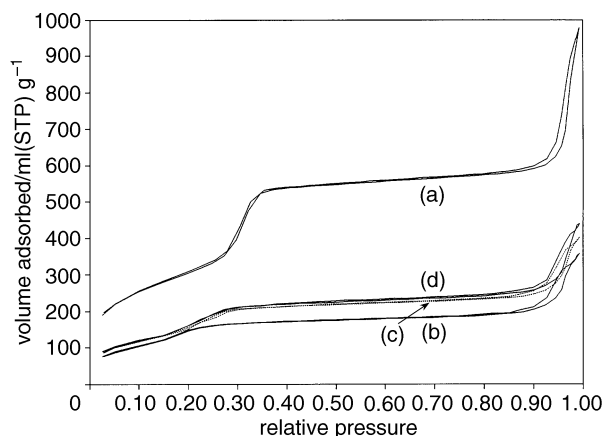


Fig. 2 Sorption isotherms of nitrogen at -196°C on (a) parent all-silica MCM-41; (b) $\text{CsLa}/\text{MCM-41A}$; (c) $\text{CsLa}/\text{MCM-41B}$ (dotted line); (d) $\text{CsLa}/\text{MCM-41C}$

Table 1 Nitrogen physisorption data of various CsLa/MCM-41 materials

sample	Si/Al ratio	impregnation method ^a	$V_p^b/cm^3 g^{-1}$	$d_p^c/\text{Å}$	BET area/m ² g ⁻¹	BET area ^d /m ² g ⁻¹
A	∞	—	0.888	36	1122	1129
B	∞	1	0.285	26	568	559
C	∞	2	0.362	31	620	564
D	∞	3 ^e	0.781	37	965	951
D	∞	3 ^f	0.387	30	660	619
E	30	—	0.922	36	1168	1169
F	30	1	0.422	32	727	654
G	30	2	0.474	36	697	643
H'	30	3 ^e	0.753	37	931	902
H	30	3 ^f	0.446	33	637	600
I	15	—	0.816	37	1023	1019
J	15	1	0.445	33	698	709
K	15	2	0.498	35	699	695
L'	15	3 ^e	0.619	36	847	818
L	15	3 ^f	0.435	33	662	658

^a 1: One-step wet impregnation, 2: solid-state impregnation and 3: two-step wet impregnation. ^b Cumulative pore volume (between $p/p_0 = 0.02$ and 0.7). ^c The mean Broekhoff-de Boer (assuming cylindrical pores) diameter.³⁴ ^d Duplicate physisorption measurements after a second re-evacuation cycle at high temperature. ^e First step of method 3. ^f Second step of method 3.

lanthanum nitrate.³⁷ The formation of CsLaO_x occurs probably after the final decomposition of lanthanum nitrate.

¹³³Cs NMR

Solid-state ¹³³Cs MAS NMR was performed to investigate the nature of Cs in the CsMCM-41 materials. Fig. 4 shows the ¹³³Cs NMR spectra of Cs⁺ ion-exchanged and CsLa/MCM-41 materials. Hydrated Cs⁺ ion-exchanged MCM-41 [Fig. 4(a)] shows a resonance at -14 ppm with a very small line-

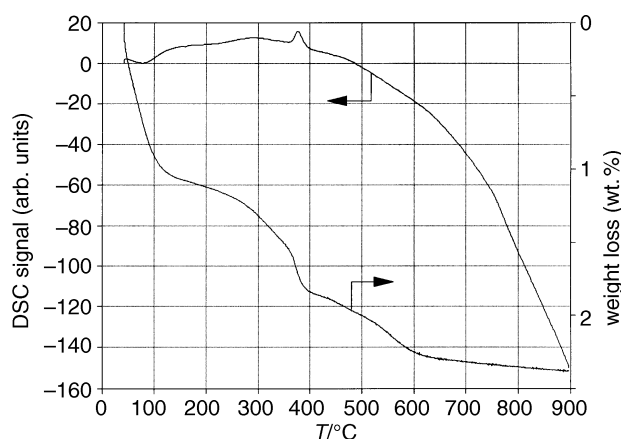


Fig. 3 DSC–TG diagram of all-silica MCM-41 impregnated with caesium acetate and lanthanum nitrate (CsLa/MCM-41A; method A)

width of 0.2 kHz. The absence of spinning sidebands indicates that the Cs⁺ cations are in a quasi-isotropic environment owing to the high mobility of the hydrated extra-framework Cs⁺ cations.^{38–42} On dehydration, the resonance shifts to -88 ppm [Fig. 4(b)] accompanied by considerable line broadening (2.4 kHz) and the appearance of spinning sidebands. This indicates that the Cs⁺ cations have lost their high mobility and now sense different chemical surroundings with their associated shielding anisotropies. The MCM-41 supported CsLaO_x [Fig. 4(d), (e)] shows a resonance between -40 and -20 ppm, depending on the Si/Al ratio of the MCM-41 support (Table 2). The nature of ¹³³Cs is probably less ionic here compared with Cs⁺ ion-exchanged MCM-41. Bulk CsLaO₂ [Fig. 4(e)] exhibits a chemical shift at -21 ppm with a linewidth at half height of 0.4 kHz. The increase of the linewidth in the supported systems suggests that the ¹³³Cs ions in CsLa mixed oxides are in a less symmetrical environment. Cs species in all-silica MCM-41 are less shielded than in the aluminosilicate MCM-41 samples and show a similar resonance, as in bulk CsLaO₂. The latter observation suggests that the Cs species have hardly any or no interaction with the silica type support. This supports the idea that lanthanum is bonded to the MCM-41 support.²⁶ The behaviour of the ¹³³Cs resonance shifting to high field by increasing the framework aluminium content, suggests that the Cs species are becoming more electropositive which results in a longer Cs–O bond.^{41,42} Considering the difference in chemical shift, there is an interaction of the AlO⁻ with the Cs⁺ cations. Broadening of the peak on increasing the aluminum content of the MCM-41 support is probably due to heteronuclear

Table 2 ¹³³Cs MAS NMR data of various Cs and La-containing MCM-41 samples

sample	Si/Al ratio	δ_{hydr}	$\Delta\nu_{1/2}^a/\text{kHz}$	δ_{dehydr}	$\Delta\nu_{1/2}^a/\text{kHz}$
bulk CsLaO ₂	—	-21	0.4		
CsLa/MCM-41A	∞	-19	1.8	-39	3.9
CsLa/MCM-41B	∞	-20, -44	1.7, 1.4	-23, -53	2.6, 2.4
CsLa/MCM-41C	∞	-20	1.8	-51	3.0
CsLa/MCM-41A	30	-29	3.2		
CsLa/MCM-41B	30	-22, -45	1.4, 1.8		
CsLa/MCM-41C	30	-29	2.8		
CsLa/MCM-41A	15	-39	2.3		
CsLa/MCM-41B	15	-22, -41	2.1, 1.9		
CsLa/MCM-41C	15	-39	1.3		
Cs-MCM-41 ^b	12	-14	0.2	-88	2.4
Cs-MCM-41 ^c	12			-55	2.4
Cs-MCM-41 ^d	12			26	8.8
Cs-MCM-41 ^e	12			48	11

^a Peak width at half height; ^b Cs⁺ ion-exchanged MCM-41; ^c 5.0 wt.% Cs; ^d 12.4 wt.% Cs; ^e 21.9 wt.% Cs.

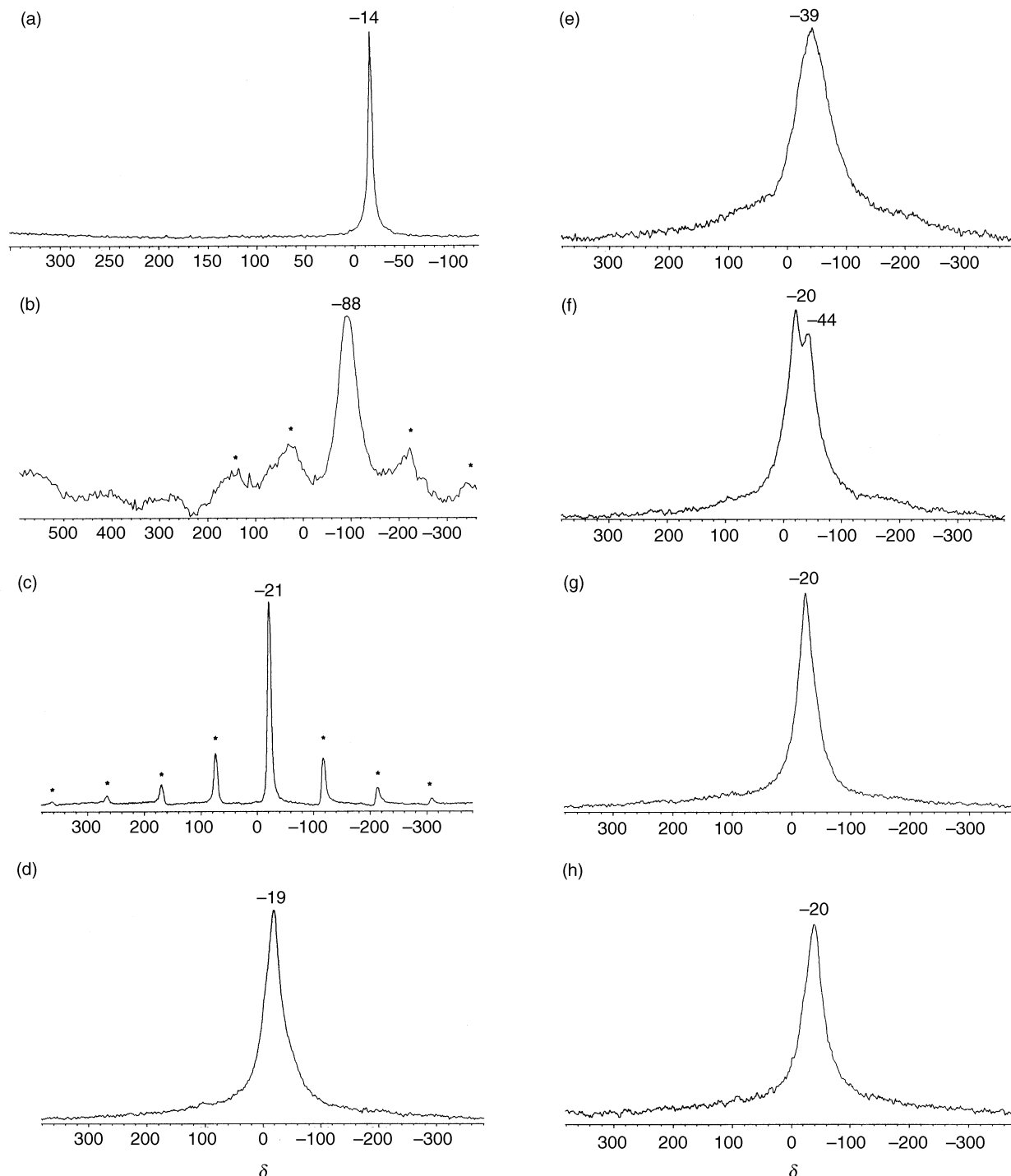


Fig. 4 ^{133}Cs MAS NMR spectra: (a) hydrated Cs ion-exchanged MCM-41; (b) dehydrated Cs ion-exchanged MCM-41; (c) bulk CsLaO_2 ; (d) $\text{CsLa}/\text{MCM-41A}$ with $\text{Si}/\text{Al} = \infty$; (e) dehydrated $\text{CsLa}/\text{MCM-41A}$ with $\text{Si}/\text{Al} = \infty$; (f) $\text{CsLa}/\text{MCM-41B}$ with $\text{Si}/\text{Al} = \infty$; (g) $\text{CsLa}/\text{MCM-41C}$ with $\text{Si}/\text{Al} = \infty$ and (h) $\text{CsLa}/\text{MCM-41A}$ with $\text{Si}/\text{Al} = 15$

dipolar coupling with the aluminium.³⁸ Studies on silica and alumina supported europium oxides show that the bonding of Eu^{3+} to SiO_2 is more covalent (less ionic) than that to Al_2O_3 .⁴³

In contrast to Cs ion-exchanged MCM-41 and $\text{CsO}_x/\text{MCM-41}$ ¹⁶ ^{133}Cs resonances of $\text{CsLa}/\text{MCM-41}$ are hardly influenced by hydration (Table 2) suggesting that the bonding of Cs^+ cations with lattice oxygen anions in the CsLa mixed oxide is stronger than that of Cs^+ with the framework oxygens in Cs^+ ion-exchanged MCM-41 [Fig. 4(a), (b)]. This is also reflected by the unaffected peak width after dehydration. Bulk CsLaO_2 is sensitive to moisture and becomes sticky upon hydration, in agreement with the reported hygroscopic

properties of CsLaO_2 .²² The insensitivity to hydration of the supported CsLa mixed oxides might be due to the interaction of the binary oxide particles with the MCM-41 framework causing a stabilization of the CsLaO_x lattice. A somewhat comparable observation is found for SiO_2 -supported NiO which is much more difficult to reduce than bulk NiO.¹⁷ It is surprising that all the $\text{CsLa}/\text{MCM-41C}$ samples show a resonance similar to that of the $\text{CsLa}/\text{MCM-41A}$ samples. This indicates that both wet-impregnation techniques lead to the same binary oxide. The prepared LaO_x layer inside MCM-41 is probably reactive enough to be converted into a CsLa mixed oxide. A comparable impregnation technique is reported for the preparation of highly dispersed BaO particles on

La₂O₃, namely impregnation of lanthana with barium nitrate followed by drying and calcination. However, the authors did not observe a BaLaO₃ phase.⁴⁴ The MCM-41-loaded samples prepared by solid-state impregnation exhibit two resonances, at -20 and -44 ppm, indicating two different Cs-containing oxides. Comparing the ¹³³Cs MAS NMR data of CsLa/MCM-41*i* (*i* = A, B and C) with those of Cs/MCM-41 a large difference in chemical shift is observed. The former shows a resonance at *ca.* -30 ppm and the latter at *ca.* +20 ppm.¹⁶ Thus, in a caesium oxide lattice ¹³³Cs is more deshielded than in CsLaO_x on MCM-41 or, in other words, shorter Cs—O bonds seem to be present.

CO₂ TPD

The basic strength and the accessibility of the basic sites of the CsLaO_x particles were measured by CO₂ temperature-programmed desorption (TPD).^{1,2,6–9,11,16} The desorption of CO₂ as a function of the temperature of several materials prepared is shown in Fig. 5. Considering ion-exchanged MCM-41, an interesting phenomenon is observed [Fig. 5 (1) and (2)]. In contrast to Cs-MCM-41, Na-MCM-41 gives a large peak at 200 °C and an amount of desorbed CO₂ (Table 3) corresponding to one molecule of CO₂ per 2 Na ions. This suggests that supported sodium carbonate-like species are formed. On the other hand, the thermal decomposition diagram of Na₂CO₃ supported on SiO₂ shows several maxima at higher temperatures. It is known that alkali-metal ion-exchanged zeolites X and Y are basic, particularly CsX, which contains a high amount of framework aluminium. Despite their basicity these zeolites show hardly any CO₂ desorption.^{1,6} The reason why Na-MCM-41 displays a large CO₂ desorption, in contrast to its moderate basicity, is probably due to the poor local crystallinity around the extra-framework Na⁺ cations and a weaker bonding of Na⁺ cations to the negatively charged framework oxygens (see ²³Na NMR data) compared with Cs⁺ cations.⁴⁵ As the Lewis base sites are considered to be oxygens adjacent to the oxygens connected directly to the extra-framework alkali-metal cations, these basic sites are more negatively charged when Cs⁺ cations are bonded at the framework. So Cs⁺ is expected to induce stronger basic sites, but probably the CO₂ probe is too large to approach these.⁴⁵ Earlier we reported that strong basic sites in MCM-41 are created by impregnation with caesium acetate followed by thermal decomposition.¹⁶ The CsLa/MCM-41A materials show a broad peak around 195 °C suggesting a lower additional basicity compared with Cs/MCM-41 (Table 3). The basicity of CsLa/MCM-41 is more

comparable to that of La/MCM-41 than to that of Cs/MCM-41 which is in accord with the fact that the basic nature of CsLaO_x has more La₂O₃ character than Cs₂O character [Fig. 5 (6) and (7)]. Energies of solution of alkali-metal dopants with oxygen-vacancy compensation correspond well with

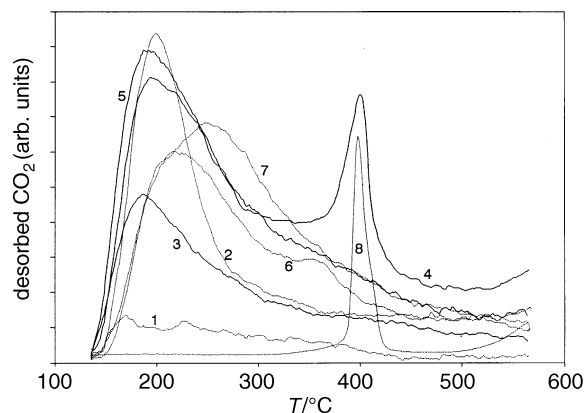


Fig. 5 TPD plots of CO₂ on various CsLa/MCM-41 (solid lines) and other basic materials (dotted lines): (1) Cs ion-exchanged MCM-41; (2) Na ion-exchanged MCM-41; (3) CsLa/MCM-41A with Si/Al = 30; (4) CsLa/MCM-41B with Si/Al = 30; (5) CsLa/MCM-41C with Si/Al = 30; (6) La/MCM-41; (7) Cs/MCM-41; (8) bulk CsLaO₂

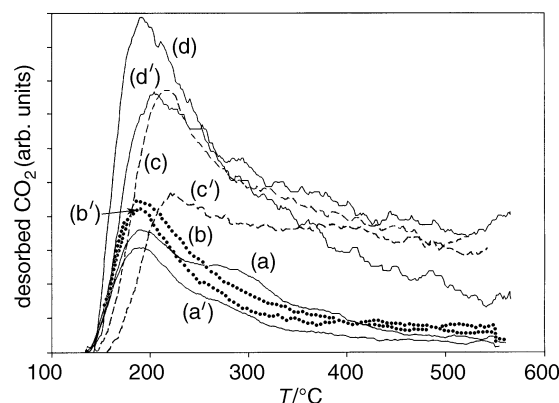


Fig. 6 TPD plots of CO₂ on various all-silica MLa/MCM-41 (M = Na, K, Rb or Cs) and their duplicate measurements (index). (a) NaLa/MCM-41; (b) KLa/MCM-41 (···); (c) RbLa/MCM-41 (---) and (d) CsLa/MCM-41A.

Table 3 CO₂ TPD data of various alkali-metal- and lanthana-containing MCM-41 materials

sample	Si/Al ratio	ratio metal per desorbed CO ₂	desorbed CO ₂ /μmol CO ₂ g ⁻¹	T _{max} /°C
Na-MCM-41 ^a	13	2.0	127	200
Cs-MCM-41 ^a	13	7.2	20	170, 250
CsLa/MCM-41A	∞	3.8	183	195
CsLa/MCM-41B	∞	5.5	110	185, 400
CsLa/MCM-41C	∞	4.6	150	190
CsLa/MCM-41A	30	9.2	72	190
CsLa/MCM-41B	30	4.0	146	195, 300
CsLa/MCM-41C	30	3.9	182	190
CsLa/MCM-41A	15	6.9	104	195
CsLa/MCM-41B	15	3.5	153	205, 400
CsLa/MCM-41C	15	8.2	87	195
La/MCM-41 ^b	∞	3.8	59	200
La/MCM-41 ^c	∞	6.2	67	200
La/MCM-41 ^d	12	8.8	123	225
Cs/MCM-41 ^e	13	4.4	159	240
Cs/MCM-41 ^f	13	13	110	270
CsLaO ₂	—	99	33	400

^a Ion-exchanged MCM-41; ^b 3.1 wt.% La; ^c 5.8 wt.% La; ^d 15.0 wt.% La; ^e 9.4 wt.% Cs; ^f 19.2 wt.% Cs.

those of binary metal oxides.⁴⁶ These calculations underline the observed basic nature of the CsLaO_x-supported MCM-41 which exhibits characteristic La₂O₃ behaviour modified by the addition of Cs₂O.

The accessibility of the CsLa mixed oxides is correlated with the amount of desorbed CO₂ per metal atom. Thereby, a reasonable correlation is achieved (Table 3) indicating that small oxide clusters are formed inside MCM-41. The stability of the CsLa mixed oxides was studied by duplicate TPD experiments. In contrast to Cs/MCM-41,¹⁶ all CsLa/MCM-41 samples show much greater stability reflected by the desorption of a similar amount of CO₂ desorbed per incorporated metal after duplicate measurements. Bulk CsLaO₂ showed one peak at 400 °C (Fig 5). The amount of desorbed CO₂ corresponds to one CO₂ per 99 metal atoms. These data are consistent with the common fact that supported metal oxides possess a lower basicity and a larger accessibility of the basic sites than bulk oxides due to the dispersity of small oxide clusters.^{17,41}

The CsLa/MCM-41B samples, prepared by solid-state impregnation at high temperature, show two maxima in the TPD diagram. One peak at 195 °C and one at 400 °C. The former peak is probably dispersed CsLa mixed oxide and the latter peak might be crystallites of XRD-invisible CsLaO₂ (*vide supra*) showing a peak comparable with bulk CsLaO₂. The tendency of metal salts to form large metal oxide particles is not uncommon during solid-state thermolysis.²⁵

Other MLa/MCM-41 systems (M = Na, K and Rb) and Na-MCM-41

The basicity of CsLa/MCM-41A was compared with that of alkali metal–lanthanum oxide containing all-silica MCM-41 (MLa/MCM-41; M = Na, K and Rb). Fig. 6(a)–(d) show the CO₂ TPD plots of MLa/MCM-41 which are normalized to the atomic weight and the duplicate measurements [Fig. 6(a)–(d)]. Desorption occurs at higher temperatures for M = Rb and Cs, indicative of a higher basicity. A strong decrease in the amount of desorbed CO₂ for the duplicate measurements suggests clustering of the oxidic particles. CsLa/MCM-41 also shows a decrease in peak intensity, but an increase in the amount of desorbed CO₂ in the higher temperature region can be observed. The profile of the CO₂ TPD plot from NaLa/MCM-41, which possesses two distinct maxima, indicates the presence of several types of oxidic species. ²³Na MAS NMR on bulk NaLaO_x and NaLa/MCM-41 revealed, indeed, different ²³Na resonances (Table 4). Beside the resonance of hydrated Na⁺ a large resonance at –6.7 ppm was observed. Rehydration of the samples occurred during transfer in the spinner. Comparing hydrated NaLa/MCM-41 with hydrated Na-MCM-41 shows that the nature of the Na⁺ ions are comparable in both materials. This suggests that hydrated NaLa/MCM-41 does not contain a NaLa mixed oxide. The small line at –2.5 ppm of hydrated Na-MCM-41 (0.3 kHz) represents an average chemical shift due to the rapid motion of the Na⁺ ions.⁴⁷ Dehydrated Na-MCM-41 shows a resonance at –13.4 ppm with a linewidth of 1.8 kHz. Considering

the large quadrupole moment and low spin number of ²³Na, it can be suggested that the latter line does not result from averaging. This indicates that in the dehydrated state the Na⁺ cation mobility is decreased drastically. RbLaO_x shows two resonances in the ⁸⁷Rb MAS NMR spectrum: a main resonance at –39.1 ppm and a shoulder at –35.5 ppm, probably due to hydration. By contrast, the CO₂ TPD profile of KLa/MCM-41 contains just one maximum, so this binary oxide might consist of one K-species. XPS studies on binary NaLa oxide and ternary NaLaNb oxide catalysts revealed that sodium is more situated as amorphous Na₂O on the surface or in the bulk of the catalysts.⁴⁸ In general it is expected that the role of Na is to poison the La₂O₃ surface.⁴⁶ The results presented for the binary KLa oxide and RbLa oxide are in agreement with reported calculations suggesting formation of an MLaO₂ (M = K or Rb) compound at a 1:1 atomic ratio.⁴⁶

In summary it can be concluded that MCM-41 is loaded with a thermally stable CsLaO_x layer structure which is independent of the wet-impregnation technique used. These mixed oxides are probably anchored on the pore walls of the support *via* La–O bonds.^{26,49} On the basis of the ¹³³Cs NMR data it might be suggested that the Cs⁺ cations are situated in the top layer of the binary oxide and not as a single surface Cs₂O species. Hereby, new basic sites are generated compared with lanthana-containing MCM-41. This hypothesis is underlined by the observation that La/MCM-41 is inactive in the base catalysed liquid phase reactions tested, in contrast with CsLa/MCM-41 (*vide infra*). Supported lanthana has the tendency to spread in a monolayer onto silica, the intraporous CsLaO_x is assumed to be dispersed in a submonolayer.^{24,27}

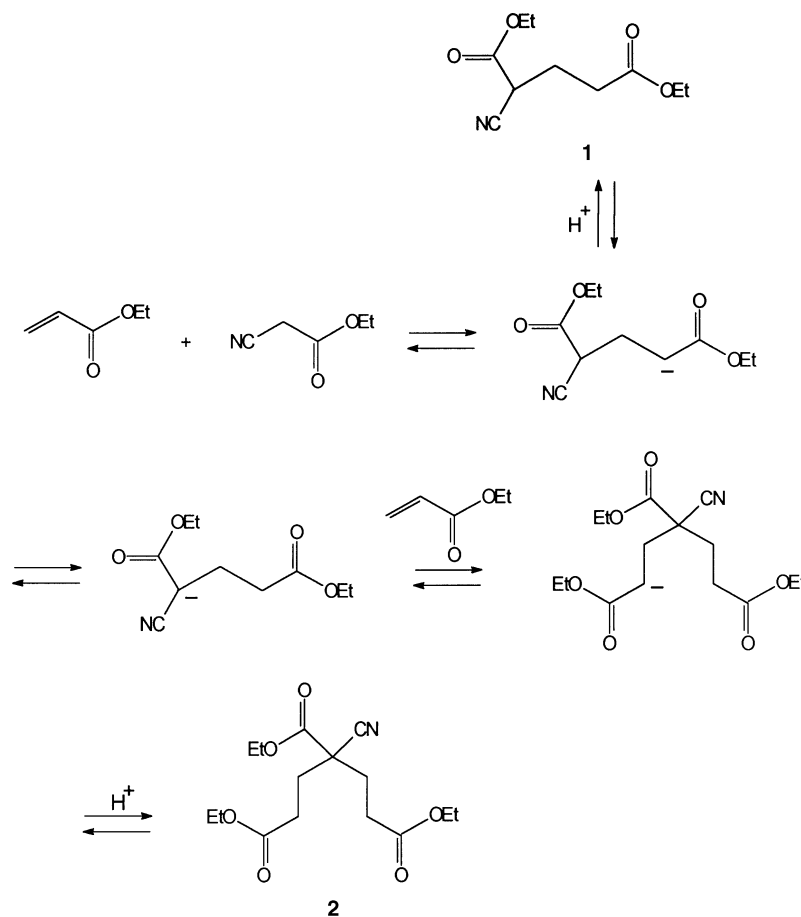
Liquid phase catalysis

The catalytic properties of the CsLa/MCM-41 materials were tested in liquid-phase Michael additions and Knoevenagel condensations. CsLa/MCM-41 catalyses the Michael addition of ethyl cyanoacetate to ethyl acrylate (Scheme 1). Besides formation of the mono-adduct **1**, compound **2**, a bis-adduct achieved by a double Michael-type addition,⁵⁰ is produced consecutively. The selectivity (at 30% m/m ethyl acrylate conversion) to **1** is slightly lower using mesoporous CsLa/MCM-41 than when applying silica-supported CsLa mixed oxide. Various catalysts can be compared by expressing their specific activity A_{wt} as mmol h⁻¹ g⁻¹. Table 5 illustrates that CsLa/MCM-41B gives a higher specific activity than the more weakly basic CsLa/MCM-41A and CsLa/MCM-41C. It is noteworthy that CsLa/SiO₂ requires a higher metal loading to achieve an activity comparable to that of CsLa/MCM-41. The highest specific activity was observed for Cs/MCM-41, but this is accompanied by a poor selectivity to both **1** and **2** due to much by-product formation. In contrast to the Knoevenagel condensation of ethyl cyanoacetate with benzaldehyde,¹⁵ Na⁺ ion-exchanged MCM-41 (Na-MCM-41) was inactive in the present Michael addition. Although the basicity of CsLa/MCM-41 is quite mild, it shows a very good performance in this reaction. This indicates that addition of CsLaO_x enhances the activity of MCM-41 substantially in the Michael addition with the poorly reactive ethyl acrylate. The anion of ethyl cyanoacetate does not react simply with α,β -unsaturated ketones; this reaction can only proceed when either the anionic intermediate is stabilized by another electronegative element or when the α,β -unsaturated ketone is sufficiently activated *via* coordination to a Lewis acid centre. The performance of CsLa/MCM-41 is ascribed to the presence of lanthanum which activates the ethyl acrylate by coordination to the ester oxygens.^{51,52} The product selectivities are probably also controlled by the mesoporous MCM-41 support. The reaction of the less activated ethyl crotonate (Fig. 7) was not achieved. However, ethyl cinnamate could be reacted in a reasonable conversion of 20% m/m after 2 h at high tem-

Table 4 ²³Na and ⁸⁷Rb MAS NMR data of hydrated Na-MCM-41 and (MCM-41 supported) MLaO_x (M = Na or Rb)

Sample	$\delta(^{23}\text{Na})^a$	$\delta(^{87}\text{Rb})^a$
Na-MCM-41 ^b	–2.5 (–13.4) ^c	
NaLaO _x	4.3, –0.2, –22.6 ^d	
NaLa/MCM-41	–6.7, –15 ^{d,e}	
RbLaO _x		–35.5, ^{d,e} –39.1
RbLa/MCM-41		not detected ^f

^a No spinning sidebands are observed. ^b Na⁺ ion-exchanged MCM-41. ^c Dehydrated Na-MCM-41 at 450 °C. ^d Hydrated alkali-metal oxide. ^e Shoulder. ^f Spectral width of 100 kHz.



Scheme 1 Double-type Michael addition of ethyl cyanoacetate to ethyl acrylate

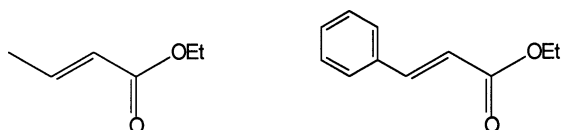


Fig. 7 Structure of ethyl crotonate (left) and ethyl cinnamate (right)

perature (160 °C; cyclohexanol as solvent). Electronic effects or shielding of the double bond by the β -alkyl/aryl group of the α,β -unsaturated ketones might be responsible for the lower activity and the observed selectivities. Pore size effects also may not be excluded as indicated by the selectivity of the reaction with ethyl cinnamate giving exclusively the corresponding mono-adduct. Pore size effects were reported earlier for Cs/MCM-41 in the double Michael addition of diethyl malonate with neopentyl glycol diacrylate.¹⁶

The basicity of CsLa/MCM-41 is too weak to catalyse the Michael addition of diethyl malonate ($pK_a = 13.3$) with ethyl acrylate under the conditions studied. This strengthens the observation that the supported CsLa oxides are not subject to leaching towards homogeneous caesium hydroxide. We noted that a stoichiometric amount of homogeneous CsOH (40 μmol of CsOH) catalyses the reaction under the same conditions within 1 h. This was, however, accompanied by a substantial amount of by-products.

The re-usability of the CsLa/MCM-41 catalysts was studied by filtering a reaction mixture, washing with acetone and re-activating the catalyst at 500 °C for 5 h. Thereby no weight loss was observed after the heating cycle. The performance of re-used CsLa/MCM-41C catalyst is given in entry 4 in Table 5. A similar A_{wt} was observed which reflects again the thermal stability of these materials during regeneration and also supports the binding assumed of the binary oxides to the MCM-41 framework.

Table 5 Michael addition of ethyl acrylate (10 mmol) and ethyl cyanoacetate (10 mmol) with either MCM-41 or SiO₂-supported caesium oxide, caesium or caesium–lanthanum oxide in refluxing ethanol at 30% m/m ethyl acrylate conversion

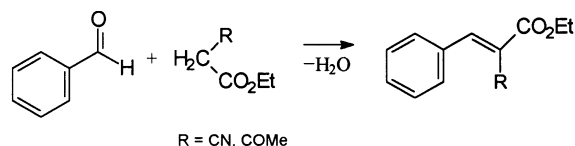
catalyst ^a	Si/Al ratio	$A_{wt}/\text{mmol h}^{-1} \text{g}^{-1}$ ^b	selectivity 1 : 2 (%) ^c
CsLa/MCM-41A ^d	∞	39.3	60 : 40
CsLa/MCM-41B ^d	∞	62.2	47 : 53
CsLa/MCM-41C ^d	∞	39.3	43 : 57
CsLa/MCM-41C ^{d,e}	∞	40.6	44 : 56
Cs/MCM-41 ^f	12	954	8 : 33 ^g
CsLa/SiO ₂ ^h	∞	32.0	64 : 36
Cs/SiO ₂ ⁱ	∞	289	36 : 42 ^g

^a 5% m/m catalyst based on total amount of substrates. ^b Specific activity at 30% m/m ethyl acrylate conversion. ^c Product selectivity at t . ^d 5% m/m Cs and 5% m/m La on MCM-41. ^e Re-used CsLa/MCM-41C catalyst after a second re-activation cycle at 500 °C for 5 h. ^f 5% m/m Cs on MCM-41. ^g Formation of by-products. ^h Cab O-sil M5 loaded with 20 wt.% of Cs metal and 20 wt.% of La metal. ⁱ Cab O-sil M5 loaded with 5% m/m Cs.

Table 6 Knoevenagel condensation of benzaldehyde with ethyl cyanoacetate or ethyl acetoacetate (R = CN or COMe, respectively) with CsLa/MCM-41, Na-MCM-41 and Cs-MCM-41 in various refluxing protic solvents

catalyst ^a	Si/Al ratio	R ^b	solvent	conversion (% m/m) ^c	A _{wt} /mmol h ⁻¹ g ^{-1 d}
CsLa/MCM-41A	∞	CN	EtOH	86	89.2
CsLa/MCM-41A	30	CN	EtOH	95	97.8
CsLa/MCM-41A	∞	CN	H ₂ O–THF	58	51.7
CsLa/MCM-41A ^e	∞	CN	H ₂ O–THF	46	54.3
CsLa/MCM-41A	30	CN	H ₂ O–THF	53	55.5
Na-MCM-41 ^f	13	CN	H ₂ O–THF	40	30.1
Cs-MCM-41 ^f	13	CN	H ₂ O–THF	55	43.3
CsLa/MCM-41A	30	COMe	H ₂ O–dioxane	21	20.7

^a 5% m/m catalyst based on total amount of substrates (10 mmol of each). ^b Reactant R = CN is ethyl cyanoacetate and R = COMe is ethyl acetoacetate. ^c Enolate conversion after 1 h. ^d Specific activity after 1 h. ^e 4% m/m re-used CsLa/MCM-41A catalyst after filtration and drying. ^f Ion-exchanged MCM-41.

**Scheme 2** Knoevenagel condensation of benzaldehyde with ethyl cyanoacetate (R = CN) or ethyl acetoacetate (R = COMe)

The Knoevenagel condensation of benzaldehyde with ethyl cyanoacetate ($pK_a < 9$) served as a study of the capability of CsLa/MCM-41 to be used in aqueous media (Scheme 2). All the CsLa/MCM-41A catalysts gave large conversions (Table 6) together with >99% selectivity to the α,β -unsaturated esters under mild conditions. Interestingly, CsLa/MCM-41A showed a better performance in ethanol than in H₂O–THF. Unexpected solvent effects were also found in the Knoevenagel condensation catalysed by silicon oxynitride⁵³ and the basic clay xonolite.⁵⁴ The former showed a higher conversion in ethanol than in THF. Xonolite however, was less active in ethanol than in water. We have reported already that the basicity of alkali-metal ion-exchanged MCM-41 was high enough to catalyse this reaction also.¹⁵ Table 6 illustrates that the specific activities A_{wt} of Na-MCM-41 and Cs-MCM-41 in H₂O–THF are a little lower than that of CsLa/MCM-41. A larger difference, *ca.* a factor 5, would be achieved if the specific activity was expressed as mol h⁻¹ mol_{al.metal}⁻¹. Weaker acidic enolates like ethyl acetoacetate ($pK_a = 10.5$; 8.0% enol)⁵⁵ could also be deprotonated under less severe conditions (solvent: H₂O–dioxane 1 : 1, 100 °C).

The re-use of the CsLa/MCM-41A catalyst is again demonstrated by a similar A_{wt} after filtration (entry 4 in Table 6) while the filtrate showed no activity. In all cases no indication of catalysis by homogeneous basic leached species was found.

The CsLa/MCM-41 materials were tested in ordinary glass reactors without taking any special precautions (CO₂-free atmosphere and dry glassware).¹ This confirms again that these MCM-41 supported CsLa mixed oxides are easy to handle, in sharp contrast with La/MCM-41. The lanthana-supported MCM-41 materials appeared to be inactive in all the mentioned liquid-phase reactions. This pertains to a much lesser extent to the earlier reported Cs/MCM-41 materials which are very active in liquid-phase catalysis, but are very moisture sensitive.¹⁶

Conclusions

Heterogeneous mesoporous stable basic catalysts are prepared by impregnation of MCM-41 with equimolar amounts of caesium acetate and lanthanum nitrate followed by drying and calcination. Loading of CsLaO_x on MCM-41 *via* solid state-like impregnation at high temperature can also be achieved. CsLa/MCM-41 materials possess small, intraporous, thermally stable CsLaO_x clusters with a submonolayer-shape

having a mild basicity. Their use as basic catalysts in aqueous media is displayed in the Knoevenagel condensation. The combination of the CsLaO_x layer and the mesoporous framework alters the product selectivity in the two-step Michael addition of ethyl acrylate and ethyl cyanoacetate. The catalysts can be re-used after a solvent flush and a high temperature cycle without loss of activity.

We thank Dr. A Sinnema for measuring and interpreting the NMR data, Mr. J.C. Groen for physisorption measurements, Dr. Y. Pluyto for DTA–TG measurements and the NIOK Institute, the Dutch School of Catalysis, for financial support.

References

- H. Hattori, *Chem Rev.*, 1995, **95**, 537 and references therein.
- D. Barthomeuf, *Catal. Rev., Eug. Sci.*, 1996, **38**, 521.
- T. Yashima, H. Suzuki and N. Hara, *J. Catal.*, 1974, **33**, 486.
- D. Barthomeuf, *J. Phys. Chem.*, 1984, **88**, 42.
- P. E. Hathaway and M. E. Davis, *J. Catal.*, 1989, **116**, 263.
- H. Tsuji, F. Yagi and H. Hattori, *Chem. Lett.*, 1991, 1881.
- M. Laspéras, H. Cambo, D. Brunel, I. Rodriguez and P. Geneste, *Microporous Mater.*, 1993, **1**, 343.
- J. C. Kim, H-X. Li and M. E. Davis, *Microporous Mater.*, 1994, **2**, 413.
- I. Rodriguez, H. Cambon, D. Brunel, M. Laspéras and P. Geneste, *Stud. Surf. Sci. Catal.*, 1993, **78**, 623.
- F. Y. N. Kanuka, H. Tsuji, H. Kita and H. Hattori, *Stud. Surf. Sci. Catal.*, 1994, **90**, 349.
- M. Laspéras, I. Rodriguez, D. Brunel, H. Gambon and P. Geneste, *Stud. Surf. Sci. Catal.*, 1995, **97**, 319.
- C. T. Kresge, M. E. Leonowicz, W. J. Roth, J. C. Vartuli and J. S. Beck, *Nature (London)*, 1992, **359**, 710.
- J. S. Beck, J. C. Vartuli, W. J. Roth, M. E. Leonowicz, C. T. Kresge, K. D. Schmitt, C. T. W. Chu, D. H. Olson, E. W. Sheppard, S. B. McCullen, J. B. Higgins and J. L. Schlenker, *J. Am. Chem. Soc.*, 1992, **114**, 10834.
- K. R. Kloetstra and H. van Bekkum, *J. Chem. Res.(S)*, 1995, 26.
- K. R. Kloetstra and H. van Bekkum, *J. Chem. Soc., Chem. Commun.*, 1995, 1005.
- K. R. Kloetstra and H. van Bekkum, *Stud. Surf. Sci. Catal.*, 1997, **105**, 431.
- J. A. Schwarz, C. Contescu and A. Contescu, *Chem. Rev.*, 1995, **95**, 477 and references therein.
- A. Kaddouri, R. Kieffer, A. Kiennemann, P. Poix and J. L. Rehspringer, *Appl. Catal.*, 1989, **52**, L1.
- R. Hoppe and S. Voigt, in *Synthesis of Lanthanide and Actinide Compounds*, ed. G. Meyer and L. R. Morss, Kluwer, Dordrecht, 1991, p. 225.
- R. K. Ungar, X. Zhang and R. M. Lambert, *Appl. Catal.*, 1988, **42**, L1.
- X. Zhang, D. A. Jefferson and R. M. Lambert, *J. Catal.*, 1993, **141**, 583.
- R. Hoppe and H. Brunn, *Rev. Chim. Miner.*, 1976, **13**, 41.
- G. M. Clark, in *The Structures of Non-Molecular Solids*, Applied Science, London, 1972, p. 254.
- Y. S. Tan, L. Q. Dou, D. A. Lu and D. Wu, *J. Catal.*, 1991, **129**, 447.
- Y-C. Xie and Y-Q. Tang, *Adv. Catal.*, 1990, **37**, 1.

- 26 A. Jentys, N. H. Pham, H. Vinek, M. Englisch and J. A. Lercher, *Microporous Mater.*, 1996, **6**, 13.
- 27 W. Grünert, U. Sauerlandt, R. Schlögl and H. G. Karge, *J. Phys. Chem.*, 1993, **97**, 1413.
- 28 J. C. P. Broekhoff and J. H. de Boer, *J. Catal.*, 1968, **10**, 377.
- 29 A. Corma, V. Fornés, M. T. Navarro and J. Pérez-Pariente, *J. Catal.*, 1994, **148**, 569.
- 30 Z. Luan, C. F. Cheng, W. Zhou and J. Klinowski, *J. Phys. Chem.*, 1995, **99**, 1018.
- 31 K. R. Kloetstra, unpublished results.
- 32 B. Marler, U. Oberhagemann, S. Vortmann and H. Gies, *Microporous Mater.*, 1996, **6**, 375.
- 33 I. V. Kozhevnikov, A. Sinnema, R. J. J. Jansen, K. Pamin and H. van Bekkum, *Catal. Lett.*, 1995, **30**, 241.
- 34 I. V. Kozhevnikov, K. R. Kloetstra, A. Sinnema, H. W. Zandbergen and H. van Bekkum, *J. Mol. Catal. A*, in the press.
- 35 K. R. Kloetstra, H. W. Zandbergen, M. A. van Koten and H. van Bekkum, *Catal. Lett.*, 1995, **33**, 145.
- 36 V. Yu, X. Feng, Z. Bu, G. L. Haller and J. A. O'Brien, *J. Phys. Chem.*, 1996, **100**, 1985.
- 37 T. C. Vaimakis, *Thermochim. Acta*, 1992, **206**, 219.
- 38 P.-J. Chu, B. C. Gerstein, J. Nunan and K. Klier, *J. Phys. Chem.*, 1987, **91**, 3588.
- 39 T. Tokuhiro, M. Mattingly, L. E. Iton and M. K. Ahn, *J. Phys. Chem.*, 1989, **93**, 5584.
- 40 D. K. Murray, J.-W. Chang and J. F. Haw, *J. Am. Chem. Soc.*, 1993, **115**, 4732.
- 41 J. T. Cheng and P. D. Ellis, *J. Phys. Chem.*, 1989, **93**, 2549.
- 42 G. E. Maciel and P. D. Ellis, in *NMR Techniques in Catalysis*, ed. A. T. Bell and A. Pines, Marcel Dekker, New York, 1994, p. 231.
- 43 J. Shen, M. J. Lochhead, K. L. Bray, Y. Chen and J. A. Dumesic, *J. Phys. Chem.*, 1995, **99**, 2384.
- 44 H. Yamashita, Y. Machida and A. Tomita, *Appl. Catal. A*, 1991, **79**, 203.
- 45 M. Huang, S. Kaliaguine and A. Auroux, *J. Phys. Chem.*, 1995, **99**, 9952.
- 46 D. J. Ilett and M. S. Islam, *J. Chem. Soc., Faraday Trans.*, 1993, **89**, 3833.
- 47 V. Laperche, J. F. Lambert, R. Prost and J. J. Fripiat, *J. Phys. Chem.*, 1990, **94**, 8821.
- 48 M. Yamamura, H. Okado, N. Tsuzuki, T. Wakatsuki and K. Otsuka, *Appl. Catal. A*, 1995, **122**, 135.
- 49 W. A. Herrmann, R. Anwender, V. Dufaud and W. Scherer, *Angew. Chem.*, 1994, **106**, 1338.
- 50 J. L. Soto, C. Seoane, A. M. Mansilla and M. C. Pardo, *Tetrahedron Lett.*, 1981, **22**, 4845.
- 51 H. Sasai, S. Arai, Y. Tahara and M. Shibasaki, *J. Org. Chem.*, 1995, **60**, 6656 and references therein.
- 52 H. Sasai, E. Emori, T. Arai and M. Shibasaki, *Tetrahedron Lett.*, 1996, **37**, 5561.
- 53 P. W. Lednor and R. de Ruiter, *J. Chem. Soc., Chem. Commun.*, 1991, 1625.
- 54 P. Laszlo, *Acc. Chem. Res.*, 1986, **19**, 121.
- 55 O. A. Reutov, I. P. Beletskaya and K. P. Butin, in *CH-Acids*, ed. T. R. Crompton, Pergamon, Oxford, 1978, p. 7.

Paper 6/06766B; Received 2nd October, 1996